Sharp Tips Produced by the Breakage of Popsicle Sticks and Their Puncture Injury Potential

Xiaoyi Hu * , Lu Li , Song Xiang , Yao Xiao , Hongchao Liu , Xuwei He , Wei Guo , Lingrong Liu

Posted Date: 7 April 2026

doi: 10.20944/preprints202604.0387.v1

Keywords: sharp tip; popsicle stick; injury; silicone film; gelatin; surrogate human tissue

 doi:10.20944/preprints202604.0387.v1

Article

Sharp Tips Produced by the Breakage of Popsicle Sticks and Their Puncture Injury Potential

Xiaoyi Hu [1,*], Lu Li [2], Song Xiang [3], Yao Xiao [4], Hongchao Liu [1], Xuwei He [1], Wei Guo [1] and Lingrong Liu [1]

[1] College of Optical, Mechanical and Electrical Engineering, Zhejiang A&F University, Hangzhou 311300, China
[2] College of Chemistry and Materials Engineering, Zhejiang A&F University, Hangzhou 311300, China
[3] Jixian Honors College, Zhejiang A&F University, Hangzhou 311300, China
[4] School of Medicine, Zhejiang University, Hangzhou, 310058, China
* Correspondence: jimhxy08@zafu.edu.cn

Abstract

Sharp tips generated by the fracture of popsicle sticks may cause human injury. This study systematically investigated the fracture behavior of popsicle sticks under different loading patterns and the associated potential risk of puncture injuries to the human body through mechanical experiments. Popsicle sticks made of *Betula platyphylla Suk.* wood were used in the experiments. Two moisture conditions (dry and wet) and three fracture loading patterns (cantilever bending fracture, three-point bending fracture, and axial compressive buckling fracture) were applied, with a total sample size of 600. Based on the geometric morphology of the fracture fragments, the hazard level was classified into Levels I, II, and III, with specific classification criteria provided. Surrogate human tissue blocks were created by simulating human skin with silicone films and subcutaneous tissue with gelatin blocks. A free-fall apparatus was employed to evaluate the penetration depth and unit energy penetration area of popsicle stick fragments into human tissues. The experimental results showed that after fracture, the number of dry specimens posing a high risk of human injury was significantly greater than that of wet specimens. The plasticizing effect of moisture on wood fibers inhibited the formation of sharp tips. The penetration risk were significantly greater for dry specimens than for wet specimens, and the inhibitory effect of moisture on puncture capability was more pronounced for smaller sharp tips. It is recommended that techniques aimed at improving the water permeability of wood be adopted to reduce the risk of puncture injuries caused by accidental fracture of popsicle sticks.

Keywords: sharp tip; popsicle stick; injury; silicone film; gelatin; surrogate human tissue

1. Introduction

Popsicle, as a globally popular frozen dessert, is consumed in enormous quantities. However, accompanying this consumption experience is a rare but severe type of injury: oral and facial puncture wounds caused by fractured popsicle sticks. These thin wooden splinters can break, especially children, bite down on them or accidentally fall, forming sharp tips that may penetrate the oral mucosa, gums, or tonsils. In extreme cases, such injuries can even threaten the airway or intracranial region. Although the clinical consequences of these injuries are well recognized, research on the mechanism by which sharp tips form on fractured popsicle sticks remains lacking, representing a gap in the field of consumer product safety.

The phenomenon of sharp tip formation during the fracture of popsicle sticks is related to the fracture behavior of wood. As a natural polymer material with anisotropic characteristics, the fracture behavior of wood is influenced by multiple factors, including wood species, loading conditions,

 doi:10.20944/preprints202604.0387.v1

microstructure, and grain direction [1]. Existing research on wood fracture mechanics has primarily focused on the mechanisms of crack initiation in wood, such as how drying stresses [2] and growth stresses [3] induce crack formation or propagation, or on the fracture behavior of wooden components under load [4,5]. However, no studies have yet investigated how sharp tips are formed during wood fracture, nor has there been research on the injury potential associated with such sharp tips.

Most existing studies on the fracture behavior of wooden components have focused on relatively large-scale elements, such as beams in timber structures [6]. However, popsicle sticks are considerably smaller, and their fracture behavior differs significantly from that of large-scale timber beams [7]. Consequently, existing theories of wood fracture mechanics are not well suited for predicting whether sharp tips will form during the fracture of popsicle sticks. Furthermore, the loading conditions under which popsicle sticks fracture also differ considerably from those of wooden structural components: the latter are subjected to specific types of loads—for instance, timber beams are typically tested under four-point bending, while columns are subjected to axial compression. In contrast, the fracture conditions of popsicle sticks are more diverse. They may break due to biting, shaking during handling, impact from accidental falls, or it may even be accidentally broken while being played with as a toy. Popsicle sticks may break due to bending deformation or instability caused by axial compression in the above fracture conditions. The probability of sharp tip formation varies across different fracture conditions, so it is necessary to conduct statistical analysis based on large sample size fracture experiments to obtain data on the likelihood of tip formation under different fracture conditions.

This study will quantitatively define sharp tips based on the geometric characteristics of the fracture surface and, with reference to existing research on knife sharpness [8], evaluate whether popsicle sticks fractured under various conditions are prone to penetrating human tissue. In this investigation, gelatin-based materials mimicking human tissue will be employed for simulation. Gelatin biomimetic materials offer advantages such as tunable mechanical properties, good biocompatibility, and low cost, and have been widely used in simulation experiments involving knife injuries [9,10].

This study aims to investigate the fracture behavior of popsicle sticks under different loading conditions and its correlation with the risk of puncture injuries, by combining wood fracture experiments with biomimetic tissue testing methods. Specifically, three fracture loading conditions—three-point bending [11], cantilever beam bending, and axial compressive buckling [12]—will be employed to quantify the probability of sharp tip formation under different fracture conditions. Concurrently, gelatin-based materials will be used to simulate human tissue, and the puncture injury potential of sharp tips will be objectively assessed by estimating the damaged area in the tissue caused by penetration per unit of puncture energy. This study seeks to elucidate the influence of fracture pattern and wood material properties on the formation of hazardous sharp tips, thereby providing a scientific basis for optimizing production processes and material selection for popsicle sticks, ultimately reducing the risk of related puncture injuries at the source.

2. Materials and Methods

2.1. Material Selection and Experimental Testing Methods

Betula platyphylla Suk. was obtained from Xiaoxing'anling mountains region in China and used as the experimental material in this study. The material was characterized by a standard air-dry density of 607 kg/m^3 [13]. Most of the popsicle sticks produced in China use this type of wood because of its excellent comprehensive performance: it is easy to process into slender sheets, has moderate strength and beautiful color, and is rich in forest resources, moderate in cost, and can meet food safety requirements. A mature popsicle stick processing industry has been formed in Yichun City, Heilongjiang Province, Dunhua City, Jilin Province, and other places, supplying products to major popsicle production enterprises across the country.

 doi:10.20944/preprints202604.0387.v1

To adapt to different sizes of popsicle, popsicle sticks are also processed into products with different sizes. In this study, popsicle sticks with a size of 125 ×14 mm and thickness of 2.0 mm were selected for investigation. In order to prevent sharp corners from harming the human body, these popsicle sticks were processed into semicircles at both ends, as shown in Figure 1a. In experiments, three different scenarios of popsicle stick fracture were simulated on a universal mechanics testing machine. These three scenarios are: (1) bending and breaking of a cantilever beam, as shown in Figure 1b, simulating the situation of holding an popsicle stick and bending and breaking it while eating popsicle; (2) Three point bending fracture, as shown in Figure 1c, simulating the situation of intentionally breaking an popsicle stick by hand; (3) Buckling fracture of axially compressed rod, as shown in Figure 1d, simulating an accidental fall while eating popsicle. The universal mechanical testing machine used in the experiment was PUYAN882 (Yaofeng Electronic Equipment Co., Ltd., Dongguan, China), with a maximum load of 5 kN and load measurement resolution of 0.01 N.

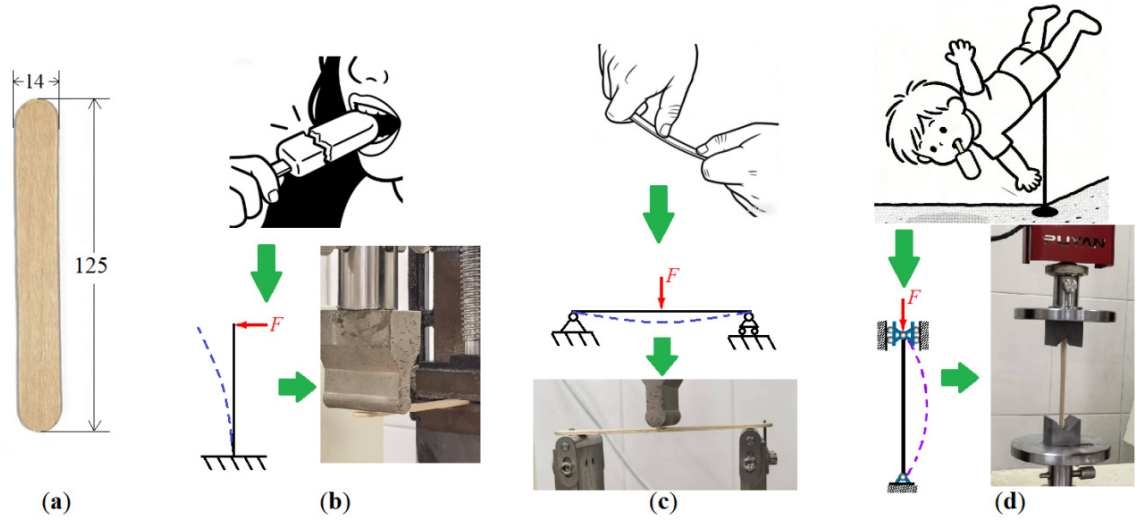

Figure 1. Size of popsicle stick and fracture loading methods used in experiments: (a) size of popsicle sticks; (b) cantilever beam bending; (c) three point bending; (d) instability bending of compression rod.

In this study, two groups of specimens with different moisture contents were compared: a dry group and a wet group. The dry group specimens were used to simulate accidental breakage when children play with dry popsicle sticks, while the wet group of specimens is used to simulate the phenomenon of accidental breakage of the popsicle stick when people eat popsicle or just finish eating popsicle (the popsicle stick has just been soaked in water in the popsicle or in the human mouth). Before experiments, the dry group specimens were stored in a specialized drying chamber, with the moisture content controlled at 12.0%±1.5%.

The wet group specimens were immersed in water prior to testing. Generally for a 125 mm long popsicle stick, there is usually a 35 mm length exposed for finger grip, and the remaining 90 mm length is buried in ice. So in experiments, only a length of 90 mm was immersed in water. The immersion time was determined based on the estimated duration that sticks remain soaked in water while people eat popsicles. 40 volunteers were participated in a test measuring the time taken to eat a popsicle and all participants provided informed consent before participating in the study. Test results are shown in Table 1.

 doi:10.20944/preprints202604.0387.v1

Table 1. Time required for eating a popsicle: statistical data from 40 volunteers.

Eating stage	Time consumed			
	Average/(s)	Maximum/(s)	Minimum/(s)	*CV*/%
1	166	308	25	36.8
2	157	305	30	37.4
Complete stage	323	530	131	26.4

Note: Eating stage 1 in the table represents the time from the start of eating until the buried part of the popsicle stick becomes exposed; Eating stage 2 represents the time from the exposure of the stick until the popsicle is fully eaten; Complete stage refers to the total time from the beginning of eating until the popsicle is completely eaten.

It should be noted that during the popsicle production process, due to the existence of quick freezing technology, although the sticks are wrapped in the popsicle, they do not have the opportunity to experience continuous and stable liquid water contact. Therefore, before popsicles were eaten, their sticks were still dry. In Eating stage 1, except for the handle portion of the popsicle stick, the rest portion of the popsicle stick is buried in the solid ice. At this time, the ice has not melted yet, so the popsicle stick is not soaked in water; At Eating stage 2, the upper part of the popsicle stick is exposed, and the exposed part of the popsicle stick will be soaked in water. It can be seen that using the statistical time of Eating stage 2 to estimate the possible soaking time of popsicle sticks in water is reasonable. Therefore, it is reasonable to use the statistical time of Eating stage 2 to estimate the possible soaking time: the average time of this stage is 157 seconds. In the experiment, for the convenience of measurement, the popsicle stick was soaked in water 150 seconds before the mechanical testing. When the predetermined soaking time was reached, the popsicle stick was quickly removed from the water and subjected to mechanical testing.

To reduce the uncertainty in experimental results caused by individual differences of specimens, a sample size of 100 was used in experiments for each control group. This study will test specimens from six control groups, each corresponding to loading and moisture conditions as shown in Table 2, with a total sample size of 600.

Table 2. Six control groups and corresponding load and moisture conditions in experiments.

Group label	Loading condition	Sample size	Moisture condition
Dry1	Cantilever beam bending	100	12.0%±1.5% MC
Dry2	Three point bending	100	12.0%±1.5% MC
Dry3	Axial compressive buckling	100	12.0%±1.5% MC
Wet1	Cantilever beam bending	100	Soak in water for 150 seconds
Wet2	Three point bending	100	Soak in water for 150 seconds
Wet3	Axial compressive buckling	100	Soak in water for 150 seconds

After fracture loading, according to the different characteristics of fracture morphology, the number of specimens with hazard levels I to III was counted for each fracture loading condition. The specific standard for dividing hazard levels is as follows:

- hazard level I: the fracture surface is relatively flat and all sharp tips have a length of less than 5 mm (excluding those with a length greater than 5 mm but the bottom cross-sectional area less than 1 mm^2);
- hazard level II: the longest sharp tip length is greater than 5 mm but less than 10 mm (excluding those with a length greater than 5 mm but the bottom cross-sectional area less than 1 mm^2);
- hazard level III: the longest sharp tip length is greater than 10 mm (excluding those with a length greater than 10 mm but the bottom cross-sectional area less than 3 mm^2).

 doi:10.20944/preprints202604.0387.v1

It should be noted that when popsicle sticks break, they will be divided into two parts. When classifying the hazard level of each broken specimen, only the part with higher hazard level or the longer one (when the hazard levels of two parts are the same) was selected for statistics, while the other part will not be analyzed. Typical examples of specimens with hazard levels I to III are shown in Figure 2a, two example of a relatively low hazard level due to the small cross-sectional area of the sharp tip is shown in Figure 2b.

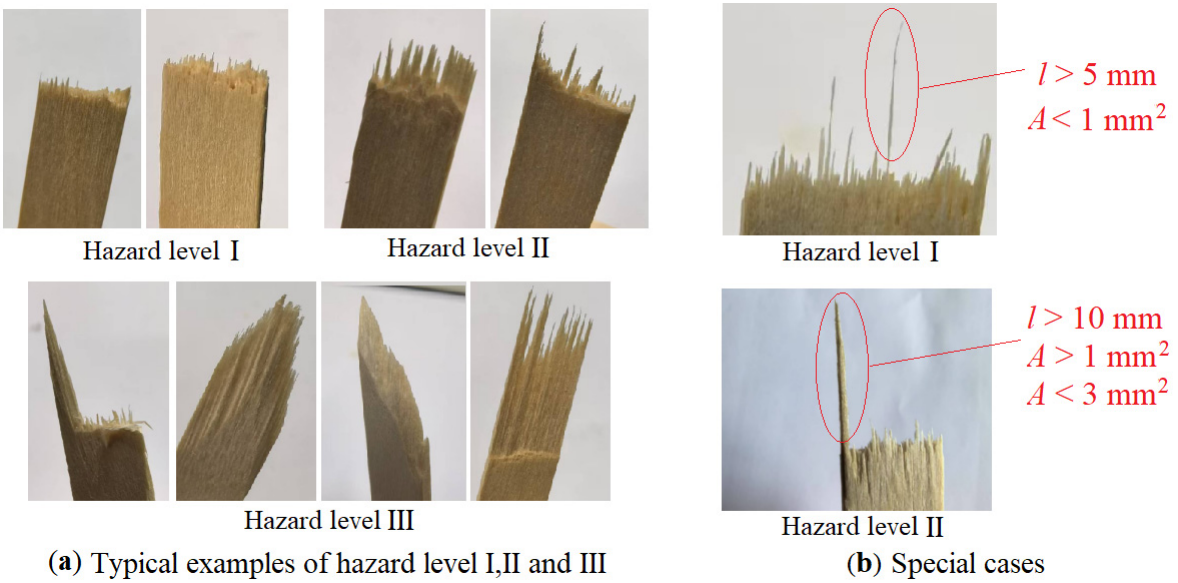

Figure 2. Hazard level classification based on fracture morphology: (a) example specimens of hazard level I to III; and (b) special cases of relatively low hazard level examples.

The classification of sharp tip lengths of 5 mm and 10 mm as the critical thresholds for II and III hazards, respectively, is based on a review of scientific literature on human skin and vascular anatomy. A synthesis of available data on epidermal thickness [14,15], dermis thickness[16,17], subcutaneous fat thickness [18], and venous depth [19,20] indicates that when the sharp tip reaches a length of 5 mm, it is capable of penetrating epidermis and dermis in most regions of human body and extending into fat layer. In extreme cases, a 5 mm sharp tip may be sufficient to puncture superficial veins, potentially resulting in severe hemorrhage. When the sharp tip reaches a length of 10 mm, it can penetrate the epidermis, dermis and subcutaneous fat layer in most areas of the body, reaching depths that may involve vital tissues and internal organs.

Following hazard level classification of the fractured specimens, 20 specimens are randomly selected from each of the three hazard level groups and further subjected to evaluation of their human injury potential. This assessment is performed by mounting each specimen into a specially designed free-fall apparatus, which enables controlled impact energy such that the sharp tip of the specimen penetrates a surrogate medium with mechanical properties analogous to human tissue. Injury potential to the human body is evaluated based on two parameters: penetration depth and penetration area per unit energy (equivalent to the wound area that can be produced in human tissue per unit of energy). A photograph of the experimental setup is shown in Figure 3a, the photo of the sharp tip piercing into the surrogate human tissue block is shown in Figure 3b, and the photo of the slider used in the experiment to pierce the broken popsicle stick into the surrogate human tissue block is shown in Figure 3c.

For all specimens, a uniform release height (h) was adopted, defined as the vertical distance between the tip of the specimen and the top surface of the surrogate human tissue block before the slider is released. During the test, the slider carrying the specimen is released from this height and falls freely, allowing the specimen to pierce into the surrogate human tissue.

 doi:10.20944/preprints202604.0387.v1

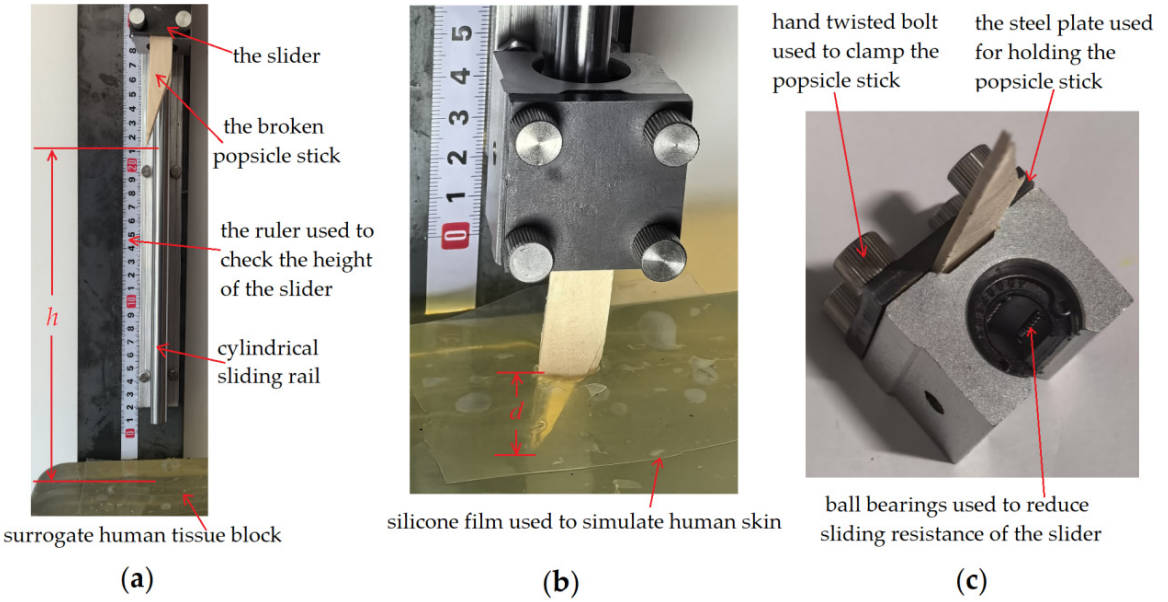

Figure 3. A photograph of the injury potential testing device and analysis method for penetration depth and penetration area of specimens: (a) overall photo of the device; (b) broken popsicle stick pierced into the surrogate human tissue block; and (c) the slider.

The height h was selected such that for the sharpest specimen, the penetration depth corresponds to 50%～80% of the thickness of the surrogate human tissue block. This ensures that for the majority of specimens, the penetration depth and penetration area are sufficiently large to be measurable, while avoiding excessive penetration that could cause the specimen to contact the metal backing plate beneath the surrogate tissue block. Based on preliminary tests and evaluations, h was set to 0.30 m.

In experiments, two key indicators were measured and recorded for each specimen: the first indicator was the depth of penetration (d), and the second indicator was the area of penetration (A). After a specimen was pierced into the surrogate human tissue block, mark the boundary between the specimen and the surrogate human tissue block surface with an ultra fine line marker pen. Digital photos of specimens after marking were analyzed by using pixel analysis software named "ImageJ" (1.54p version, Wayne Rasband and contributors, National Institutes of Health, USA) to extract two indicators: penetration depth and penetration area. After obtaining the penetration depth d and penetration area A of specimens, unit energy penetration area A_I is further calculated using the following formula:

$$A_1 = \frac{A}{W(h+d)} \quad (1)$$

Where A is the penetration area of the specimen into the surrogate human tissue block; W is the weight of the slider (W = 1.63 N); h is the release height of the slider (h = 0.30 m) and d is the penetration depth of the specimen into the surrogate human tissue block.

It should be noted that during testing, the fractured specimen was fixed to the slider and freely dropped to pierce into the surrogate human tissue block. The weight of different fractured specimens varies, however the weight of all fractured specimens are less than 0.01 N, far less than the weight of the slider. Therefore, for the sake of convenience, the weight of the fractured specimen carried on the slider was ignored when calculating energy.

Surrogate human tissue blocks were composed of a 55 mm thick gelatin block that simulates subcutaneous tissue, covered with a 0.30 mm thick silicone film to simulate human skin. For a replacement of human subcutaneous tissue, 10% gelatin blocks composed of a 1:9 ratio of gelatin (Hefei Bomei Biotechnology Co., Ltd., Xinghua International Plaza, No. 50 Hetang Road, Luyang District, Hefei City, 250 g bloom) to water by mass were used [21,22]. Considering that the mechanical properties of gelatin materials are significantly affected by temperature, the gelatin block is placed in

 doi:10.20944/preprints202604.0387.v1

a constant temperature chamber 24 hours before the experiment, and the temperature is set at 10.0℃. The constant temperature chamber used by the research group is HWS-30 (Supo Instrument Co., Ltd., Shaoxing, China), the temperature control range is 0-75℃, with a temperature fluctuation of ± 0.5℃.

It should be noted that the structure of human skin and subcutaneous tissue is very complex, consisting of many different layers, and the mechanical properties of different skin layers are also different [23,24]. The model in the experiment needs to be as simple as possible. If only gelatin is used in the model to simulate human tissue, without the protection of skin, the depth and area of penetration will be too large, which is seriously inconsistent with the actual situation. Therefore, models that mimic human tissue must include skin. However, the difficulty and cost of creating a surrogate human tissue block that includes different skin layers are too high. Taking into account the above factors, a layer of silicone film was chosen to simulate human skin in the experiment. This not only avoids making the model difficult to prepare, but also makes the experimental results closer to the real situation. The 0.3mm thick silicone film used is thinner than most parts of the skin in the human body, and this thickness is closer to the skin thickness of the most vulnerable parts of the human body. Therefore, the results of the experiment represent the worst-case scenario of human injury.

2.2. Data Analysis Methods

In this study, the energy required for each ice cream stick to break (encompassing maximum, minimum, average values), as well as the depth and area of the ice cream stick penetrating the simulated human tissue block, were the most critical experimental data. In order to quickly calculate the fracture energy of each fractured specimen, the research team has developed a dedicated mini program. This program can directly read the load displacement data output by the universal mechanical testing machine, and numerically integrate the experimental data to obtain the value of fracture energy. This approach enhanced the automation level of data analysis, accelerated the processing speed, and reduced the manual workload involved in data analysis.

In addition to calculating fracture energy, analyzing digital images is also crucial. The acquisition of relevant data on how deep the sharp tip penetrates the surrogate human tissue block and the area of the penetration, as well as the maximum cross-sectional area of the sharp tip bottom used for hazard level classification of broken popsicle sticks are all based on the analysis of digital photos. This study used ImageJ software to analyze digital images and obtain the required data. This study used ImageJ software to analyze digital images and obtain the required data. Figure 4a summarizes the analysis process of penetration depth and penetration area, while Figure 4b summarizes the analysis process of the bottom area of the sharp tip.

Preprints.org (www.preprints.org) | NOT PEER-REVIEWED | Posted: 7 April 2026 doi:10.20944/preprints202604.0387.v1

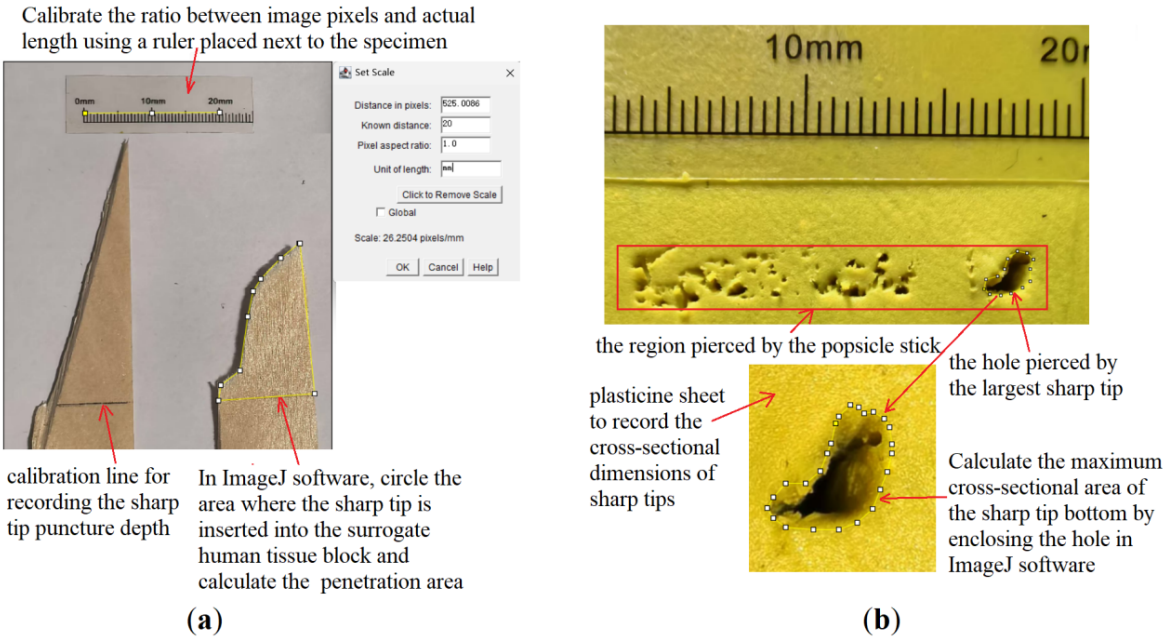

Figure 4. Using ImageJ software to calculate key experimental indicators: (a) penetration depth and area; (b) the bottom area of the sharp tip.

Beyond the analyses of fracture energy, penetration depth, and penetration area described above, statistical analyses were conducted on the data from 600 specimens using Origin 2024. Box plots were created to compare the distribution of fracture energy among the different control groups, and the Tukey post hoc test was used to evaluate the significance of statistical differences between groups.

3. Results

The fracture energy of six control groups, the number of specimens and the mean fracture energy for each hazard level are listed in Table 3. Results for the Tukey post hoc test of fracture energy comparing six different groups and comparing hazard level I to III specimens in each group is also listed in the table.

Table 3. The fracture energy of six control groups, the number of specimens and the mean fracture energy for each hazard level.

Group	Fracture energy/(J)		Number of specimens			Mean energy/(J)	
label	Max,Min,Ave	Tukey	I	II	III	I, II, III	T-in-group
Dry1	0.683, 0.277, 0.453	CD	85	6	9	0.455, 0.455, 0.434	AAA
Dry2	0.733, 0.361, 0.513	C	69	13	18	0.524, 0.491, 0.479	AAA
Dry3	1.257, 0.335, 0.786	A	30	42	28	0.819, 0.838, 0.675	AAB
Wet1	0.648, 0.301, 0.444	D	79	15	6	0.447, 0.444, 0.408	AAA
Wet2	1.373, 0.273, 0.695	B	83	11	6	0.689, 0.669, 0.836	AAA
Wet3	1.443, 0.225, 0.852	A	58	31	11	0.890, 0.798, 0.795	AAA

The data in the table indicate that the fracture energy required for popsicle sticks to break varies depending on the fracture pattern. The cantilever beam pattern (Dry1 and Wet 1 group) requires the lowest fracture energy, while the axially compressed buckling pattern (Dry 3 and Wet 3 group) requires the highest fracture energy. However, the Tukey post hoc test results show that for dry popsicle sticks, the fracture energy required for Dry1 group is not significantly different from that required for Dry2 group (the analysis results for these two pattern are labeled CD and C, respectively;

 doi:10.20944/preprints202604.0387.v1

sharing the same letter C indicates no significant difference). In contrast, the fracture energy of Dry3 group (labeled A) differs significantly from Dry1 and Dry2 group. For wet popsicle sticks, the fracture energy of the three groups differ significantly from one another (labeled D, B, and A, respectively). When comparing dry and wet popsicle sticks under the same fracture pattern, except for Dry2 vs. Wet2 group, where the difference in fracture energy is significant (labeled C and B, respectively), the differences for Dry1 vs. Wet1 group (labeled CD vs. D) and Dry3 vs. Wet3 group (labeled A vs. A) is not significant.

For the specimens in each control group, the Tukey post hoc test provided comparisons of fracture energy among specimens classified into the three human injury hazard levels. The results show that, with the exception of the Dry3 group, where the outcome was AAB—indicating that the fracture energy of hazard level III specimens was significantly lower than that of hazard level I and hazard level II specimens—the other five groups all yielded AAA results, indicating no significant differences in fracture energy among specimens of different hazard levels.

In addition to fracture energy, the table also lists the number of specimens at hazard levels I, II, and III for each control group. The experimental data show that among dry groups, Dry3 group had the highest number of specimens classified as high human injury risk (hazard level III), while Dry1 group had the lowest number of specimens in the high-risk category. The comparison of experimental data between dry and wet group reveals that after fracture, the number of specimens with a high hazard level in wet groups is significantly lower than that in dry groups.

Figure 5 is the box plot of fracture energy for six experimental control groups. As can be seen from the plot, the box lengths and whisker lengths of the three control groups Dry1, Dry2, and Wet1 are significantly smaller than those of Dry3, Wet2, and Wet3, indicating that the fracture energy dispersion of these three groups is relatively small.

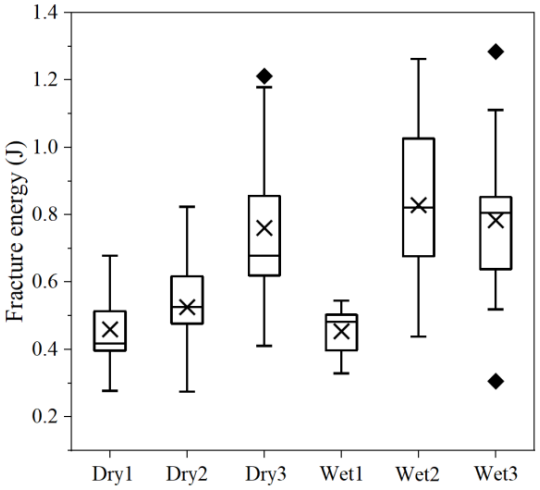

Figure 5. Box plot of fracture energy for six experimental control groups.

It can also be observed that data outliers appear in Dry3 and Wet3. This is because the fracture pattern of both control groups is related to axial compressive buckling fracture pattern. Since this fracture pattern is associated with the loss of equilibrium, the possible range of force when it loses balance is relatively large, which further leads to increased uncertainty in fracture energy.

Figure 6 is the box plot of three hazard level specimens for each of the six control groups. In this figure, control groups with same fracture patterns are represented by the same box color. It can be seen that the degree of data dispersion in fracture energy for specimens at different human injury hazard levels varies across fracture patterns. Under the cantilever bending fracture pattern (Dry1 and Wet1 groups), the box length for hazard level I specimens is relatively short, but the whisker length is relatively long, indicating that although the fracture energy of hazard level I specimens has a wide overall range, most of the values are concentrated. In contrast, hazard level II specimens show the

 doi:10.20944/preprints202604.0387.v1

opposite pattern: the box length is relatively long while the whisker length is short, suggesting that the fracture energy values are more evenly distributed. For hazard level III specimens, a considerable difference in data dispersion is observed between dry and wet specimens.

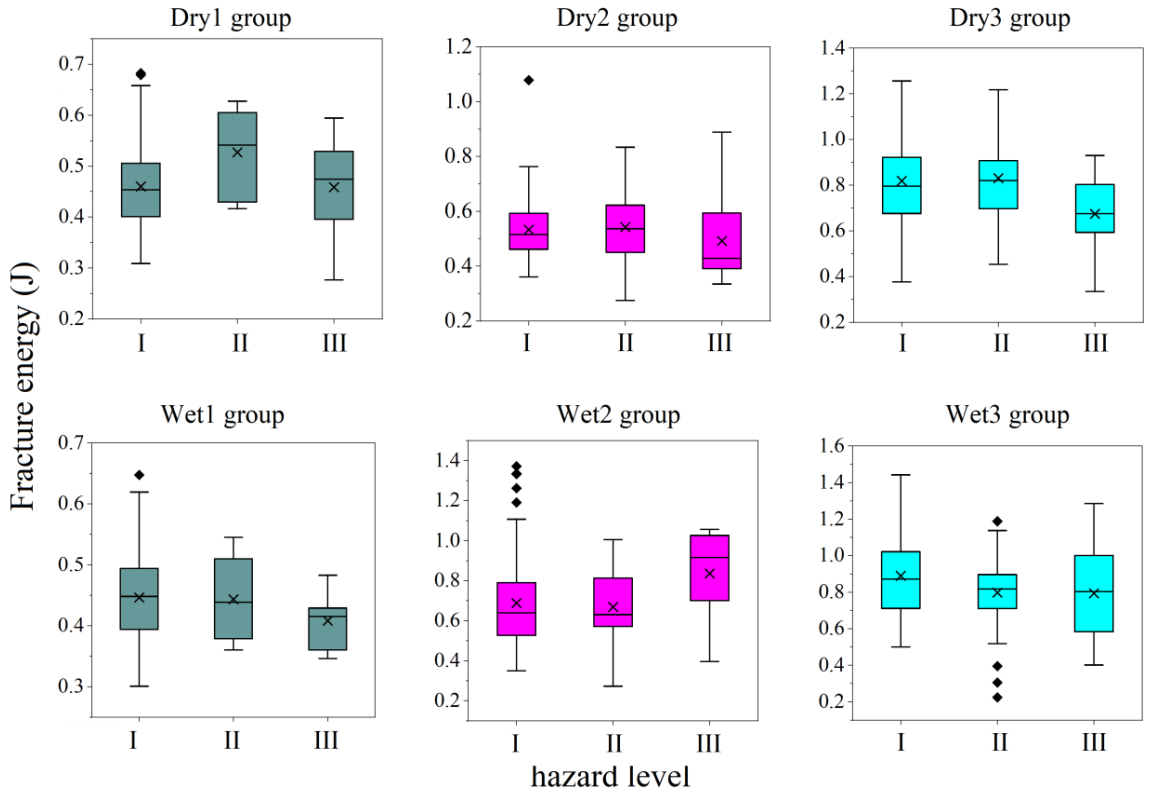

Figure 6. Box plot of three hazard level specimens for each of the six control groups.

Under the three-point bending fracture pattern, the differences in fracture energy among the three hazard levels are not pronounced. The only notable difference is that the fracture energy of wet specimens is significantly higher than that of dry specimens. This is because under this fracture pattern, the deflection of wet specimens at fracture is substantially increased, thereby requiring more energy to break.

Under the axial compressive buckling fracture pattern, among the three hazard levels for dry specimens, the difference between hazard levels I and II is not significant, while the fracture energy of hazard level III specimens is lower. This indicates that under this fracture pattern, popsicle sticks that fracture earlier (i.e., those that break with less energy consumption) are more likely to pose a greater risk to human safety.

Observing the outlier data points in the figure, it can be seen that hazard level I specimens are the most prone to producing outliers, while no outliers are observed among hazard level III specimens. This may be related to the fact that hazard level I specimens have the largest total number and hazard level III specimens have the smallest total number; with a larger sample size, the probability of generating outliers increases.

Table 4 listed penetration depth and unit energy penetration area of specimens with different hazard levels. It can be seen that specimens of hazard level III exhibit significantly greater penetration depth and penetration area per unit energy than those of hazard level II, while hazard level II specimens in turn show substantially greater values than hazard level I specimens. This indicates that the method proposed earlier in this paper for classifying hazard levels based on the geometric morphology of fractured popsicle sticks is effective.

 doi:10.20944/preprints202604.0387.v1

Table 4. Penetration depth and unit energy penetration area of specimens with different hazard levels.

Hazard level	Water regime	Penetration depth /(mm)			Unit energy penetration area/(mm²)		
		max	min	ave	max	min	ave
1	dry	3.2	0	0.2	23	0	1
	wet	0	0	0	0	0	0
2	dry	13.8	0	7.7	105	0	61
	wet	13.1	0	2.9	72	0	12
3	dry	38.6	5.5	23.9	596	105	361
	wet	35.0	3.3	16.0	560	43	209

It should be noted that during experiments, all hazard level III specimens were able to pierce into the surrogate human tissue block, and the vast majority of hazard level II specimens were also able to pierce into. However, only a very small number of hazard level I specimens pierced into the surrogate human tissue block; most were rebounded and failed to penetrate. For those specimens that failed to penetrate, both penetration depth and penetration area were recorded as zero.

Considering that the vast majority of specimens at hazard level I cannot penetrate the surrogate human tissue block, but specimens above hazard level II can penetrate, scatter plots were drawn for the penetration depth and unit energy penetration area of hazard level II and III to conduct a more in-depth analysis of the experimental data. Figure 7 is a scatter plot of the penetration depth and unit energy penetration area of a hazardous level III specimen into a surrogate human tissue block.

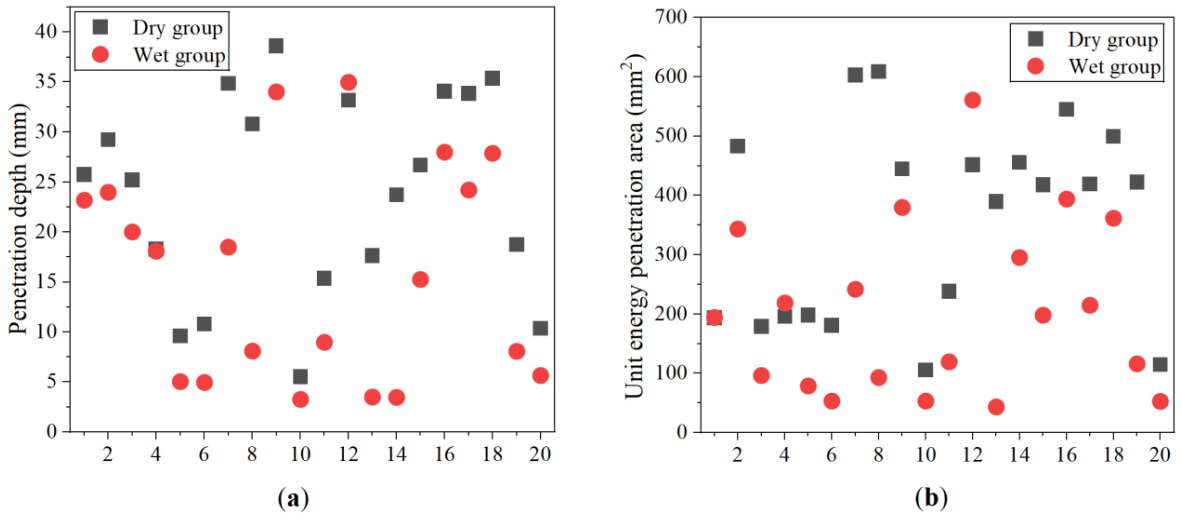

Figure 7. Scatter plot of simulated human injury data for specimens with hazard level III pierce into a surrogate human tissue block: (a) penetration depth; and (b) unit energy penetration area.

As can be seen from the plot, both the penetration depth and the penetration area per unit energy are generally significantly greater for dry specimens than for wet specimens. This is because after being soaked in water, the sharp tips of the popsicle sticks become soft and are prone to bending deformation upon contact with the surface of the surrogate human tissue block, thereby increasing the resistance to penetration and consequently reducing both the penetration depth and the penetration area per unit energy.

It should be noted that in the experiment, a dry specimen was first pierced into the surrogate human tissue block. Afterwards, soak the same specimen in water for 150 seconds and conduct the test again. Because the same specimen is used, each scatter point in the figure (represented by black and red dots) corresponds to the same specimen, resulting in stronger comparability. The experimental results indicate that, except for a very small number of specimens (such as specimen

 doi:10.20944/preprints202604.0387.v1

No. 4), the penetration depth is slightly deeper when wet, while the rest of the specimens penetrate deeper when dry.

Figure 8 is a scatter plot of the penetration depth and unit energy penetration area of a hazardous level II specimen into a surrogate human tissue block.

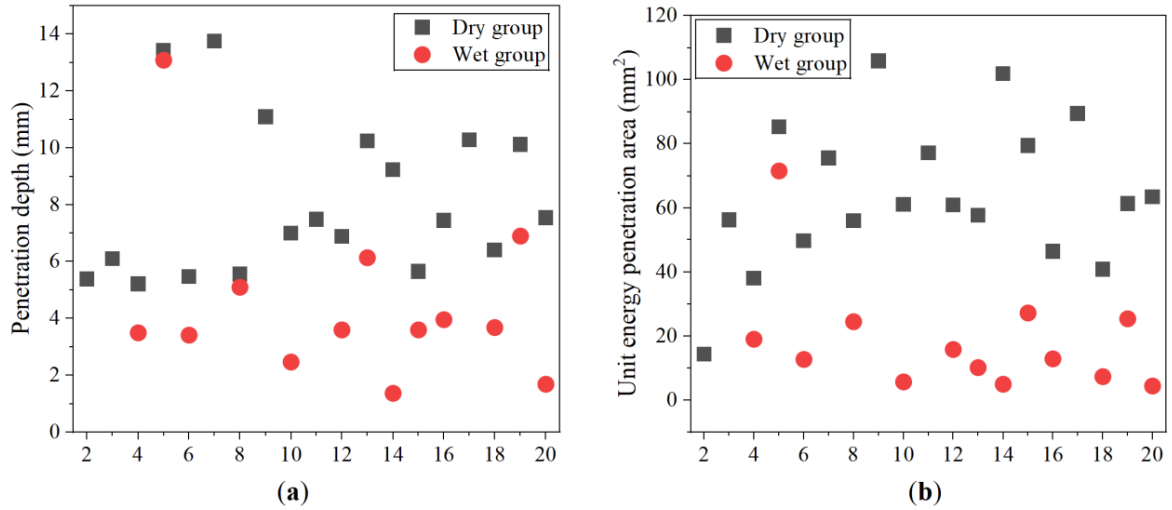

Figure 8. Scatter plot of simulated human injury data for specimens with hazard level II pierce into a surrogate human tissue block: (a) penetration depth; and (b) unit energy penetration area.

As can be seen from the plot, the trend that dry specimens exhibit greater penetration depth and penetration area than wet specimens is entirely consistent with that observed for hazard level III specimens. However, the difference is that the disparity between dry and wet specimens is more pronounced for hazard level II specimens. This is because the sharp tips of hazard level II specimens are significantly smaller than those of hazard level III specimens. Consequently, when soaked in water, the sharp tips of hazard level II specimens are more readily and fully saturated, becoming "softer." This leads to a more substantial effect on the penetration performance of hazard level II specimens after water soaking compared to that of hazard level III specimens.

4. Discussion

4.1. Fracture Energy and Risk of Human Injury

From the perspective of fracture energy, the cantilever bending fracture requires the least energy to break a popsicle stick, followed by three-point bending fracture, while axial compressive buckling fracture demands the highest fracture energy. This difference primarily stems from the distinct stress distribution mechanisms within the popsicle stick under different loading conditions. In cantilever beam bending fracture process, the bending moment increases progressively toward the clamp, so most of the deformation energy must be absorbed by the region (high tensile stress region and high compression stress region) near the clamp, see Figure9a. As a result, the volume of wood available to absorb energy is very limited, leading to the lowest fracture energy. Under this fracture pattern, fracture typically occurs near the clamp, producing relatively clean and neat fracture surfaces without generating large sharp tips. Therefore, the number of specimens classified as high-risk is the smallest. This loading mode—which corresponds to the real-life scenario of breaking a popsicle stick by applying force with one's fingers while eating a popsicle—is the easiest way to fracture the stick, but it also poses the least risk of injury to the human body.

 doi:10.20944/preprints202604.0387.v1

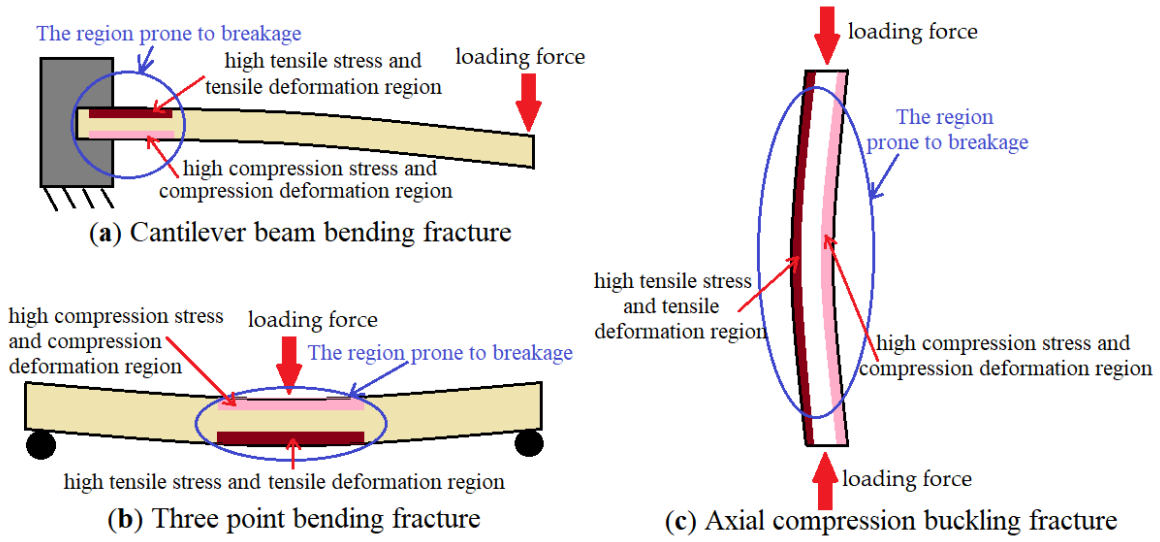

Figure 9. The main regions where deformation energy is consumed during the fracture process of popsicle sticks (high compression stress zone and high tensile stress zone): (a) cantilever beam bending fracture; (b) three point bending fracture; and (c) axial compressive buckling fracture.

In three-point bending fracture, the bending moment in the popsicle stick increases toward the central loading point. Since there are adjacent regions on both sides of the loading point, the volume of the stick available to absorb deformation energy is larger than that in the cantilever bending configuration, see Figure 9b. Consequently, more deformation energy can be absorbed during the fracture process, resulting in a slightly higher fracture energy for three-point bending fracture compared to cantilever bending fracture. In practice, unless force is deliberately applied to the popsicle stick at three points, fracture in the three-point bending pattern rarely occur.

In axial compressive buckling fracture, the popsicle stick is subjected to a "pure bending state" along its entire length. As a result, high-stress regions develop across the surface of the entire stick, with one side undergoing tensile deformation and the opposite side undergoing compressive deformation, see Figure 9c. The total volume of material participating in the deformation is significantly larger than in the other two loading configurations, enabling the stick to absorb a greater amount of energy through deformation. Therefore, this fracture pattern yields the highest fracture energy. Achieving fracture in this manner requires a substantially greater force than in the previous two cases. In real-life scenarios, this fracture pattern typically occurs only when a person accidentally falls while eating a popsicle, and the impact forces the stick to fracture in this way. This fracture pattern also poses the highest risk of injury. Experimental results indicate that this fracture pattern produces the largest number of specimens classified as high-risk. To reduce the likelihood of such accidental falls, it is advisable to avoid walking or running while eating a popsicle.

4.2. The Influence of Moisture on the Formation of Sharp Tips

Although the difference in fracture energy between dry specimens under three-point bending fracture and cantilever bending fracture was not statistically significant (Tukey's test result: C vs. CD), a comparison between dry and wet specimens under the same fracture pattern revealed that the fracture energy of wet specimens was not consistently lower than that of dry specimens. In fact, under three-point bending fracture, wet specimens exhibited even higher fracture energy. This phenomenon is closely associated with the significantly increased deflection of wet specimens during three-point bending, suggesting that moisture not only reduces the strength of the material but may also alter its fracture toughness.

Regarding the relationship between fracture morphology and hazard level, dry popsicle sticks had a significantly higher number of high-risk (hazard level III) specimens than wet ones. This

 doi:10.20944/preprints202604.0387.v1

indicates that the plasticizing effect of moisture on wood fibers effectively inhibits the formation of sharp tips, thereby reducing the likelihood of generating long, sharp fragments after fracture. Further analysis showed that among dry specimens subjected to axial compressive buckling, hazard Level III specimens were the most numerous, and their fracture energy was significantly lower than that of Level I and Level II specimens. This implies that specimens that fracture earlier are more prone to producing high-risk sharp tips. This finding has important engineering implications: when designing similar thin wooden products, attention should not be limited to strength, stiffness, and ease of use; rather, it is essential to control their fracture behavior under accidental loading to avoid the formation of sharp tips.

The difference in puncture performance between dry and wet specimens further reveals the influence of moisture on the mechanical behavior of sharp tips. Scatter plots show that dry specimens exhibited significantly greater puncture depth and penetrated area per unit energy than wet specimens. The primary reason is that the sharp tips of wet specimens become softer upon absorbing water, making them more prone to bending and deformation upon contact with the tissue surface, thereby increasing puncture resistance. Notably, this phenomenon was more pronounced in Level II specimens than in Level III specimens, because the smaller sharp tips of Level II specimens absorb water more fully, resulting in a more obvious softening effect. This finding suggests that moisture has a stronger inhibitory effect on the puncture capability of smaller sharp tips. However, previous experimental results also indicated that, in a few isolated cases, the puncture capability of sharp tips slightly increased under wet conditions. Given the low probability of this phenomenon, the current research methods could not determine the cause of this enhanced puncture performance. It is speculated that it may be related to low water permeability in those particular tips, making them less affected by moisture, or to a lubricating effect of water during the puncture process.

In summary, whether a fractured popsicle stick produces high-risk sharp tips depends not only on the loading pattern but also on the moisture content of the wood. In the dry state, popsicle sticks are more likely to generate long, sharp fragments under axial compressive buckling, posing a higher risk of puncture injury. In the wet state, the plasticizing effect of moisture on wood fibers significantly reduces both the probability of sharp tip formation and the puncture capability. Therefore, from a product safety design perspective, it is recommended that material processing techniques for popsicle sticks aim to improve their water permeability, thereby reducing the risk of sharp tip formation following accidental fracture in the dry state. Additionally, parents should pay special attention to children playing with dried popsicle sticks after consuming ice cream, to prevent minor accidents from leading to serious injuries.

4.3. The Validity and Limitations of This Study

This study represents the first attempt to investigate the potential harm of popsicle stick penetration into the human body using mechanical experimental methods. A hazard classification method based on the geometry of fracture fragments was proposed, with specific classification criteria established. The study revealed that, under different loading patterns, the number of fracture fragments at various hazard levels differs. Furthermore, surrogate human tissue blocks were used to simulate the severity of injury caused by penetrating fragments of different hazard levels.

The loading mechanisms involved in popsicle stick fracture were examined using steel clamps to apply constraints and a steel loading head to apply loads. This experimental setup is easy to implement and offers good repeatability. However, this loading configuration differs from the actual loading conditions under which popsicle sticks fracture in real-world scenarios. The fracture conditions of popsicle sticks in real-world scenarios are far more variable, and the sticks typically fracture while in direct contact with the human body and under loads applied by human body. Human tissues, such as fingers or oral mucosa, have a low elastic modulus and are prone to significant deformation, which stands in stark contrast to the steel indenter and clamps, which have a very high elastic modulus and undergo minimal deformation. Consequently, when a popsicle stick

 doi:10.20944/preprints202604.0387.v1

fractures under real loading conditions, the contact area is larger, and the resulting fracture behavior differs from that observed in the experiments.

Moreover, measurements of penetration depth and penetrated area per unit energy depend on the specific thickness and mechanical properties of human tissues. In the experiments, 0.3 mm thick silicone film was used to simulate human skin, which differs from actual skin. The mechanical properties of the 10% gelatin used in the experiments also differ from those of real human tissues. The mechanical behavior of human tissues varies significantly due to factors such as age, sex, ethnicity, and lifestyle. Therefore, the data obtained in this study can only serve to demonstrate that fractured popsicle sticks have the potential to cause puncture injuries of varying severity; they cannot be used to quantitatively assess actual harm to the human body, such as the real penetration depth or the actual area of tissue penetration.

5. Conclusion

This study systematically investigated the fracture behavior of popsicle sticks under different loading patterns and its potential impact on the risk of puncture injuries to the human body, using a combination of mechanical experiments and surrogate tissue testing. The main conclusions are as follows:

(1) Significant differences in fracture energy were observed among the three loading patterns: cantilever bending required the lowest fracture energy, three-point bending was intermediate, and axial compressive buckling required the highest. This difference arises from the distinct stress distribution patterns within popsicle sticks under each loading configuration.

(2) Dry popsicle sticks exhibited a significantly higher number of high-risk (hazard level III) specimens than wet ones. The plasticizing effect of moisture on wood fibers effectively inhibits the formation of sharp tips, thereby reducing the likelihood of generating long, sharp fragments after fracture. Under axial compressive buckling fracture, dry specimens produced the largest number of hazard level III specimens, and their fracture energy was significantly lower than that of hazard level I and hazard level II specimens, indicating that specimens that fracture earlier are more prone to producing high-risk sharp tips.

(3) Puncture test results showed that dry specimens exhibited significantly greater penetration depth and penetrated area per unit energy than wet specimens. Under wet conditions, the sharp tips become softer upon water absorption and are prone to bending deformation upon contact with the tissue surface, thereby increasing puncture resistance. This phenomenon was more pronounced in hazard level II specimens than in hazard level III specimens, indicating that moisture has a stronger inhibitory effect on the puncture capability of smaller sharp tips.

(4) This study proposes, for the first time, a hazard classification method based on the geometric morphology of fracture fragments and validates its effectiveness. However, because the experiments employed steel fixtures and surrogate tissue materials whose mechanical properties differ from those of real human tissues, the data obtained can only serve to demonstrate the relative puncture potential of fragments at different hazard levels and cannot be directly used to quantitatively assess actual human injury.

Based on the above conclusions, it is recommended that material processing techniques for popsicle sticks aim to improve their water permeability, thereby reducing the risk of sharp tip formation following accidental fracture in the dry state. Additionally, parents should pay special attention to children playing with dried popsicle sticks after consuming popsicle.

 doi:10.20944/preprints202604.0387.v1

Author Contributions: Conceptualization, X.H. (Xiaoyi Hu); methodology, X.H. (Xiaoyi Hu), L.L.(Lu Li) and H.C.(Hongchao Liu); software, X.W. (Xuwei He); validation, X.H. (Xiaoyi Hu); formal analysis, X.H. (Xiaoyi Hu); investigation, X.H. (Xiaoyi Hu), S.(Song Xiang) and Y.(Yao Xiao); resources, X.H. (Xiaoyi Hu) and L.L.(Lu Li); data curation, X.H. (Xiaoyi Hu), H.C.(Hongchao Liu), W.(Wei Guo) and L.R. (Lingrong Liu); writing—original draft preparation, X.H. (Xiaoyi Hu); writing—review and editing, X.H. (Xiaoyi Hu); visualization, X.H. (Xiaoyi Hu) and W.(Wei Guo); supervision, X.H. (Xiaoyi Hu); project administration, X.H. (Xiaoyi Hu); funding acquisition, X.H. (Xiaoyi Hu) and L.L.(Lu Li). All authors have read and agreed to the published version of the manuscript.

Funding: This research was funded by the National Natural Science Foundation of China, grant number 32171700.

Informed Consent Statement: Informed consent was obtained from all subjects involved in the study.

Data Availability Statement: The original contributions presented in this study are included in the article. Further inquiries can be directed to the corresponding author.

Acknowledgments: The corresponding author of the paper expresses gratitude to all colleagues and collaborators who supported the research, as well as to their families for their support of the paper work.

Conflicts of Interest: The authors declare no conflict of interest. The funders had no role in the design of the study, in the collection, analyses, or interpretation of data, in the writing of the manuscript, or in the decision to publish the results.

References

1. Su,Q.;Liu,W.H.;Ma,X.J.;Zhang,J.C.;Yu,Z.H.;Liu,Z.X.;Zhao,D.X. A nonlinear elastic-plastic model describing the bending and fracture behavior of Caragana korshinskii Kom. branch wood. *Wood Mater. Sci. Eng.* 2025, 20,1277-1287.
2. Florian,B.;Maximilian,A.;Markus,L.;Josef,F. Prediction of moisture-induced cracks in wooden cross sections using finite element simulations. *Wood Sci. Technol*.**2023**,*57*, 671–701.
3. Hu, X.Y.; Liu, Z.L.; Zhuang, Z. XFEM study of crack propagation in logs after growth stress relaxation and drying stress accumulation. *Wood Sci. Technol*. **2017**,*51*, 1447–1468.
4. Tu,J.C.; Zhao, D.; Zhao, J.; Zhao, Q. Experimental Study on Crack Initiation and Propagation of Wood with LT-Type Crack Using Digital Image Correlation (DIC) Technique and Acoustic Emission (AE). *Wood Sci. Technol.* **2021**, *55*, 1577–1591.
5. Romanowicz,M.;Grygorczuk,M. The effect of crack orientation on the mode I fracture resistance of pinewood. *Int J Fract*. 2024,248,27-48.
6. Zhang,B.Z.; Xie,Q.F.; Xue, J.Y. Study on the flexural behavior evolution of timber beams with natural shrinkage cracks in historic timber structure.*Structures***2025**, *73*, 108429.
7. Guo,F.; Altaner, C.M.; Jarvis, M.C. Thickness-dependent stiffness of wood: potential mechanisms and implications. Holzforschung. 2020,74,1079-1087.
8. Schuldt,S.; Arnold,G.; Kowalewski, J.; Schneider, Y.; Rohm, H. Analysis of the sharpness of blades for food cutting [J]. Journal of Food Engineering, 2016,188,13-20.
9. Bolliger, S.A.; Wallace, E.; Dobay, A.; Knaute, D.F.; Thali, M.J.; Barrera, V. The cutting edge—an investigation into the pressure necessary for cutting skin with different knife blade types. Int J Legal Med. 2020, 134,1133-1140.
10. Schaerli, S.; Schulz, R.; Gascho, D.; Enders, M.; Baumann, S.; Thali, M.J.; Bolliger, S.A.; Injury potential of thrown sharp kitchen and household utensils. Forensic Sci Med Pathol. 2018,14,31-41.
11. Siegel, C.; Buchelt, B.; Wagenführ, A. Application of the three-point bending test for small-sized wood and veneer samples. *Wood Mater. Sci. Eng*. 2022,17,157-162.
12. Yoshihara,H.; Maruta, M. Critical load for buckling of solid wood elements with a high slenderness ratio determined based on elastica theory. *Holzforschung*, 2022,76, 179-187.

 doi:10.20944/preprints202604.0387.v1

13. Cheng,J.Q.; Yang,J.J.; Liu,P. Characteristics and Utilization of Wood. In Chronicle of Chinese Timber, 1st ed.; China Forestry Publishing House: Beijing, China, 1992; pp. 143–144.
14. Lintzeri,D.A.; Karimian, N.; Blume-Peytavi, U.; Kottner, J. Epidermal thickness in healthy humans: a systematic review and meta-analysis. J Eur Acad Dermatol Venereol. 2022,36,1191-1200.
15. Chopra,K.; Calva, D.; Sosin, M.; Tadisina, K.K.; Banda, A.; Cruz,C.D.L.; Chaudhry,M.R.; Legesse,T.; Drachenberg,C.B.; Manson,P.N.; Christy,M.R. A comprehensive examination of topographic thickness of skin in the human face. Aesthet. Surg. J. 2015,35:1007-1013.
16. Oltulu, P.; Ince, B.; Kokbudak, N.; Findik, S.; Kilinc, F. Measurement of epidermis, dermis, and total skin thicknesses from six different body regions with a new ethical histometric technique. Turkish Journal of Plastic Surgery, Turk J Plast Surg. 2018,26,56-61.
17. Oltulu,P.; Tekecik, M.; Tekecik, Z.T.; Kilinc, F.; Ince, B. Measurement of epidermis, dermis, and total skin thicknesses from six different face regions. Selcuk Med J. 2022,38,210-215.
18. Störchle, P.; Müller, W.; Sengeis, M.; Lackner, S.; Holasek, S.; Furhapter-Rieger, A. Measurement of mean subcutaneous fat thickness: eight standardised ultrasound sites compared to 216 randomly selected sites. Sci Rep. 2018,8,16268.
19. Matsumoto, M.; Tateishi, A.; Kobayashi, H.; Hashiguchi, N. Vein depth and diameter as predictive indicators of visibility and palpability during venipuncture in healthy volunteers. PLOS One. 2025, 20,e0323367.
20. Brandt, H.G.S.; Jepsen, C.H.; Hendriksen, O.M.; Lindekær, A.; Skjønnemand, M. The use of ultrasound to identify veins for peripheral venous access in morbidly obese patients. Dan Med J. 2016,63,A5191.
21. Kneubuehl,B.P.; Rothschild, M.A.; Thali, M.J.; Coupland, R.M. General wound ballistics. In Wound Ballistics-Basics and Applications, 2nd ed.; Kneubuehl,B.P.,Eds.; Publisher: Springer, Berlin, Germary, 2011, pp.38.
22. Park,N.R.;Kim,K.H.;Mo,J.S.;Yoon,G.H. An experimental study on the effects of the head angle and bullet diameter on the penetration of a gelatin block. 2017,106,73-85.
23. Joodaki, H.; Panzer M.B. Skin mechanical properties and modeling: A review. *J. Eng. Med.* 2018,232,323-343.
24. Kuilenburg, J.V.; Masen, M.A.; Heide, E.V.D. Contact modelling of human skin: What value to use for the modulus of elasticity? *J.Eng.Tribol.* 2012,227:349-361.